Investigation Into MI52 Septa Wire Failures

M. Backfish

March 23, 2017

1 Introduction

This document describes four mechanisms which can damage an electrostatic septa. It attempts to offer a simple form to model these effects in order to better understand the potential impact to the septa. In the first section a simplified form of the Bethe-Bloch equation is applied to Tungsten in order to estimate the power potentially deposited within a beam spill from Fermilab's Main Injector and the resultant temperature increase. In the second section we use Poisson Superfish to get a better idea of what happens as wires are lost at the extremities of the Septa and how this change in electric field could contribute to increased breakage. Section three deals with potential electromagnetic induced heating as a result of the close proximity to the high intensity proton beam. The last section deals with residual gases within the beam pipe which can interact with the primary beam and cause the release of both electrons and ions. These ions can then be accelerated within the high voltage field of the septa.

2 Energy Deposited in the wire by the beam

2.1 Relativistic Bethe Bloch Equation

This document describes how to utilize the stopping power in the Bethe-Bloch equation to determine energy lost while a particle travels through matter. This will be applied to Tungsten. The calculations used in this section use a simpler form which is valid within the limit $2\gamma m_e << M$ as described in [1]. The units and variables used in Table 2 are taken directly from Reference [1].

$$E_{total} = E_{kin} + E_0 \tag{1}$$

$$\gamma = \frac{E_{total}}{E_0} \tag{2}$$

$$\beta = \sqrt{1 - \left(\frac{1}{\gamma}\right)^2} \tag{3}$$

Symbol	Meaning	Value or Units
K	$4\pi N_A r_e^2 m_e c^2$	0.307 $MeV cm^2 mol^{-1}$
N_A	Avagadro's number	6.022 x $10^{23} mol^{-1}$
r_e	Classical electron radius	2.818 fm
$m_e c^2$	Electron mass	0.5110 MeV
M	Projectile mass	MeV
z	Projectile charge	unitless (units of e)
Z	Atomic number of absorber	unitless (units of e)
A	Atomic mass of absorber	$gmol^{-1}$
I	Mean excitation energy	MeV
ρ	Absorber density	gcm^{-3}

Table 1: Table of parameters used for the equations 5 and 6 taken directly from source [1] .

Using equations 1, 2, and 3, β can be written in terms of the kinetic energy, E_{kin}, as shown in equation 4. The PDG states, "Moderately relativistic charged particles other than electrons lose energy in matter primarily by ionization and atomic excitation." The Betha-Bloch equation is used to describe this energy loss or stopping power [2]. The form shown in equation 5 is written in terms of the units shown in table 2 and uses the form outlined in source [1]. By using β from equation 4 one can write equation 5 in terms of the kinetic energy. Note the units for kinetic energy in table 2 are MeV. The term $\frac{dE}{dr}$ is related to $\frac{dE}{dX}$ by a factor of the density as shown in equation 6.

$$\beta = \sqrt{1 - \left(\frac{1}{\frac{E_{kin}+E_0}{E_0}} \right)^2} \tag{4}$$

$$-\frac{dE}{dr} = K * z^2 * \rho * \frac{Z}{A} * \frac{1}{\beta^2} \left(Ln \left[\frac{2 * m_e * C^2 * \beta^2 * \gamma^2}{I} \right] - \beta^2 \right) \tag{5}$$

$$\frac{dE}{dr} * \frac{1}{\rho} = \frac{dE}{dX} \tag{6}$$

Figure 1 shows plots of equation 6 versus the kinetic energy. This equation proves to be in good agreement with tables from the software PSTAR which is maintained by NIST. PSTAR is often used by the high energy physics community for determining stopping power [4].

The Particle Data Group manual quotes the Tungsten stopping power, or $\frac{dE}{dX}$, for a minimum ionizing particle at 1.145 $\frac{MeV cm^2}{g}$ [2]. Using equation 6, which applies all of the above equations, we find Tungsten's stopping power for an 8 GeV proton is 1.34 $\frac{MeV cm^2}{g}$ and the stopping power for a 120 GeV proton is 1.97 $\frac{MeV cm^2}{g}$.

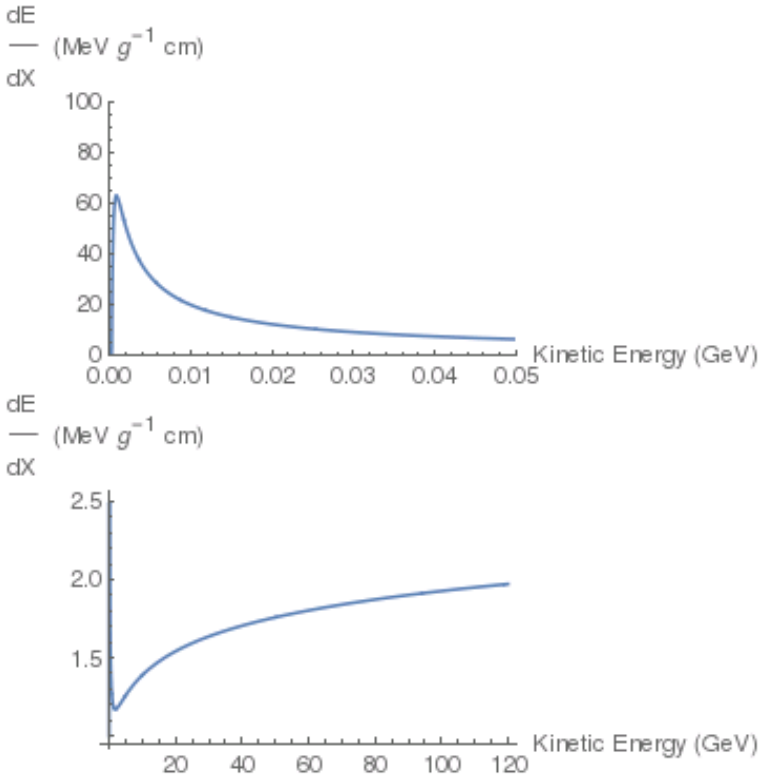

Figure 1: Plotting $\frac{dE}{dX}$ for Tungsten across two different ranges of kinetic energy

2.2 Deposited Heat in a Wire

Symbol	Meaning	Value or Units
$Energy_{perProton}$	Energy Deposited Per 120000 $MeVProton$	MeV
$W_{perProton}$	Power Deposited Per Proton In Watts	Watts
$\frac{dE}{dX}$	Stopping Power of Tungsten	1.97 $\frac{MeVcm^2}{g}$
L	Length traveled in Wire $\frac{4r}{\pi}$	cm
ρ	Tungsten/Absorber density	19.3 $\frac{g}{cm^{-3}}$
Q	Heat transferred into Septa Wire	$Joules$
ΔT	Temperature Change in Septa Wire	$Kelvin$
N	Number of Protons	$1E13$ $Protons$
C	Absorber Specific Heat (Heat Capacity)	0.13 $\frac{J}{g*K}$
$\mathcal{E}$	Absorber Thermal Conductivity	0.85 $\frac{W}{cm*K}$
r	Absorber/Wire Radius	.00508 cm
$length$	Absorber/Wire Length	4.1275 cm
m	Absorber/Wire Mass	0.0065 $grams$
$SuperCycle$	SuperCycle Time	60 $Seconds$
P	Power	$Watts$
A	Cross Sectional Area of wire	$Watts$

Table 2: Table of parameters used for the equations 5 and 6 taken directly from source [1] .

All variables for this section are defined in table 2. The energy deposited in an absorber can be described by equation 7.

$$Energy_{perProton} = \frac{dE}{dX} * \rho * L \tag{7}$$

L, or the distance traveled through the wire, is a bit trickier. One could assume the wire is a cube and just set L equal to the diameter of the wire, or to be more precise we can determine the average length of all of the parallel chords that bisect a circle of that diameter. Equation 8 is a function describing the length of a chord of a circle as a function of the angle created by a radius drawn from each of the chord endpoints. Using the mean value theorem for integrals we obtain equation 9. Thus the average path length that a particle will travel through a septa wire is described by $\frac{4r}{\pi}$ and equation 7 becomes equation 10.

$$f(\theta) = 2rSin(\frac{\theta}{2}) \tag{8}$$

$$\frac{1}{2\pi - 0}\int_0^{2\pi} 2rSin(\frac{\theta}{2})d\theta = \frac{4 * r}{\pi} \tag{9}$$

$$Energy_{perProton} = \frac{dE}{dX} * \rho * \frac{4 * r}{\pi}(MeV) \tag{10}$$

Equation 10 is in MeV so using the conversion factor of $\frac{1.6*10^-13\ Joule}{1\ MeV}$ we find $3.94 * 10^{-14}$Joules deposited in a septa wire per proton.

Assuming every extracted Proton during one beam spill, $N = 1*10^{13}\ Protons$, travels through the first Septa wire we obtain equation 11 and a total power deposited, Q, of .394 Joules.

$$Q = Power_{perProton} * N \tag{11}$$

Equation 12 relates the heat transferred to an object, Q, to its specific heat, C. Rewriting it in terms of the change in temperature gives us an equation that describes the increase in temperature of a septa wire as a result of one spill of protons using the very conservative estimate that each of those protons travels through the wire once. Piecing it all together we estimate a 466 Kelvin increase in temperature as a result of one slow spill from the Main Injector if each Proton traveled through the wire. This assumes no heat loss through conduction or radiation.

$$Q = mC\Delta t \tag{12}$$

$$\Delta t = \frac{Q}{mC} \tag{13}$$

Averaging the energy Q from above over a full superscycle, 60 $Seconds$, as in equation 14 results in a power of .007 $Watts$. Fourier's Law, otherwise known as the Law of Heat Conduction, can be used to estimate the steady rise in temperature as a result of this energy. According to this law heat can be conducted according to Equation 15 where A is the cross section area of the wire and length is the length of the wire. Replacing Heat Conducted with P for power per supercycle and Solving for ΔT results in equation 16. Note the additional factor of $\frac{1}{2}$ added to account for the fact that heat can be dissipated both directions. This results in a change in temperature of 196.861 $Kelvin$ due to conduction out of the septa wire.

$$P = \frac{Q}{SuperCycle} \tag{14}$$

$$HeatConducted = \mathcal{E}A\frac{\Delta T}{length} \tag{15}$$

$$\Delta T = \frac{P * length}{2A\mathcal{E}} \tag{16}$$

Both models above over simplify the scenario with regards to how many Protons actually travel through the first Septa wire. First of all, each Proton passes the wires far more that one time in the path to the Fixed target experimental areas. Secondly, the machine uses half integer extraction which results in transverse particle deviations that alternate around the centroid every other orbit with an ever increasing amplitude each orbit. If the step size is tuned up correctly most particles will actually step right over the wires. This unknown flux is the largest problem with this model.

3 Electrostatic Field Model Using Superfish

While trouble shooting recent septa wire failures, the question arose as to what happened to the field on the remaining wires as wires from the ends broke. To better understand this phenomena a simplified 2 dimensional Poisson Superfish model was created that shows a simple geometry with and without end wires. Figure 2 shows these results with all of the wires, while figure 3 shows the results when wires are removed. The second portion of each of these figures shows a plot of the electric field along a line that travels through each of the wires. In both figures the wires are kept at ground potential while the cathode, the lower most surface is kept at $100,000\ Volts$. Equipotential lines are plotted in pink in the first parts of the figures. It is clear from these simulations that as wires break, the electric field increases on the remaining wires. A higher electric field will subject these end wires to higher forces and could result in an increased rate of breakage over time.

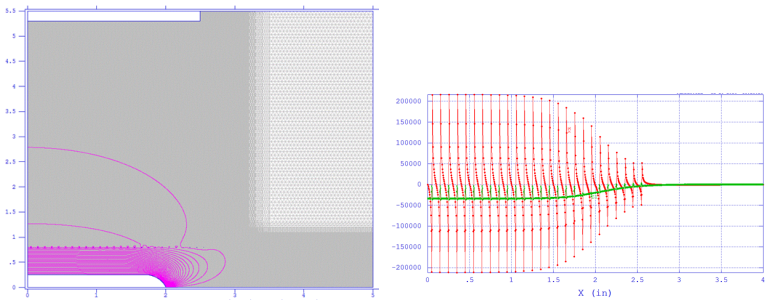

Figure 2:

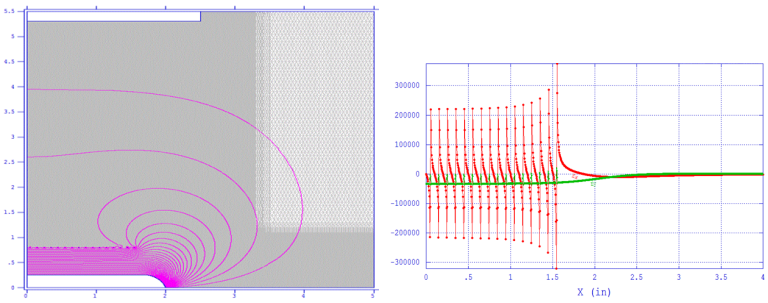

Figure 3: With fewer wires at the end of the septa, electric field will increase on the remaining wires thus increasing the force on these wires.

4 Electromagnetic Induced Heating as a Result of the Close Proximity to the High Intensity Proton Beam

In 2012 as CERN pushed the SPS to higher intensities in order to satiate the LHC's extreme thirst for Protons, they started to break flying wires [6]. The SPS is a 450 GeV machine. Previously in 2002 they had found that RF modes in the wires and scanner tanks ultimately led to heating [5] while running 2 *batches* of 72 *bunches* with $1.1 * 10^1 1$ $\frac{protons}{bunch}$. This is $15.8 * 10^{12}$ $Protons$. The wires acted as antenna and could be broken. The heating was heavily dependent on the bunch length. These breaks could occur while the wires were in the parked position, meaning totally outside of the interaction of primary beam. They modeled the behavior on a test stand using wires and currents to test the system. Ultimately in 2002 they added ferrites to the system to damp the damaging RF modes [6]. In 2012 they found that they had to add additional damping wires to damp RF modes during measurements while the beam was actually striking the wire.

I have yet to find a good way to model these effects to determine whether we could be breaking wires as a result of RF modes. These breaks have occurred as we ramped up the Main Injector beam intensity to deliver 700 KW to Nova experiments. We now run over $50 * 10^{12}$ Protons to the Numi target every 1.333 $Seconds$.

Learning to model and characterize heating effects due to RF coupling will likely be very important as we chase the intensity frontier.

5 Heating Due to Residual Gas Interactions in the Presence of a High electric Field

It is believed that any heating caused by the beams interactions with residual gases would result in wires breaking evenly throughout the length of the MI52 Septa. With this in mind, the beam's interaction with residual gases is not a likely candidate for answering why wires are breaking from the end of the Septa. With this in mind, wire Septa are often built with Ion Clearing electrodes, which the MI52 Septa tanks do not have.

The stopping power, or $\frac{dE}{dX}$ of air is $1.815 \frac{MeV cm^2}{gram}$ for a MIP as taken from the PDG [2]. As shown earlier during the discussion of Bethe Bloch, the stopping power of a MIP should be within a factor of 2 of $\frac{dE}{dX}$ for a 120 GeV Proton. The air density at sea level is $.001225 \frac{grams}{cm^3}$. The vacuum inside the septa is $1 * 10^-9$ Torr. One atm of air pressure is 760 Torr, so to determine the density of air in the beam pipe scale the density at sea level by the vacuum pressure in the beam pipe over 760 Torr as in equation 17. Next using equation 7, the density determined in equation 17, ,a Septa length of 304.8 cm, and the conversion from MeV to Joules we find that the power deposited in the septa vacuum vessel per

Proton is $1.4 * 10^{-}25$ *Joules*.

To determine how many Protons travel through the Main Injector we will make some estimates. During Numi beam operations the beam is in the Main Injector for about .7 *Seconds*. With an orbit period of about $11 * 10^{-6}$ *seconds* and a beam intensity of about $50 * 10^{12}$ this results in about $3 * 10^{18}$ Protons passing through the Septa for each Numi cycle. For slow spill with its cycle time for beam in the Main Injector of about 4.25 *seconds* and an intensity of about $5 * 10^{12}$ Protons per cycle the number of protons through the septa is more like $2 * 10^{18}$.

Using the power per Proton determined above we find about $4.5 * 10^{-7}$ *Joules* are deposited in the residual gas for Numi beam across the entire Septa and about $2.75 * 10^{-7}$ *Joules* for the slow spilled beam. This number is very low and not likely to contribute to any wire heating.

This does not account for any mechanisms in which trapped ions and electrons can be multiplied through acceleration to the cathode thus causing a release of secondary electrons.

It should be noted that resonances can occur that result in electron cloud formations within the beam pipe. These clouds have been monitored in the Main Injector [7] in the MI52 region just downstream of the extraction septa. Retarding Field Analyzers or RFAs are used to measure the transverse traveling electrons which escape the beam pipe. Those electrons first encounter a wire mesh screen which can be biased to prevent electrons from escaping. Figure 4 shows data from four different RFAs: I:CLOUD1, I:CLOUD2, I:CLOUD3 and I:CLOUD4 along with the bias voltage, I:CLDV1, Main Injector Ion Pump, IP521C and the Main Injector Septa position, I:ES52AU. This plot was made during a bias voltage scan. The electron cloud signals suddenly increased. It was determined that septa were moved in preparation for injecting beam into the Tevatron.

This picture shows that there is a relationship between septa position and both vacuum and electron cloud formation. Electrons are released when the beam interacts with residual gases thus providing seed electrons for electron cloud formation. This shows that while the residual gas interactions might not be high enough to deposit any substantial energy into wires, there are other mechanisms that can add more current. Any electrons with transverse momentum could pass over the grounded wires of the septa and be accelerated to a kinetic energy of 100 KeV before striking the cathode. At that point secondary emission off the cathode would dictate how many electrons and ions were released. Any positive ions would quickly be accelerated back to the septa wires. A detailed model of this effect is needed to truly account for whether or not the beam interacting with residual gases could cause wire breakage.

$$.001225 \ \frac{grams}{cm^3} * \frac{1 * 10^{-9} \ Torr}{760 \ Torr} = 1.6 * 10^{-15} \ \frac{grams}{cm^3} \tag{17}$$

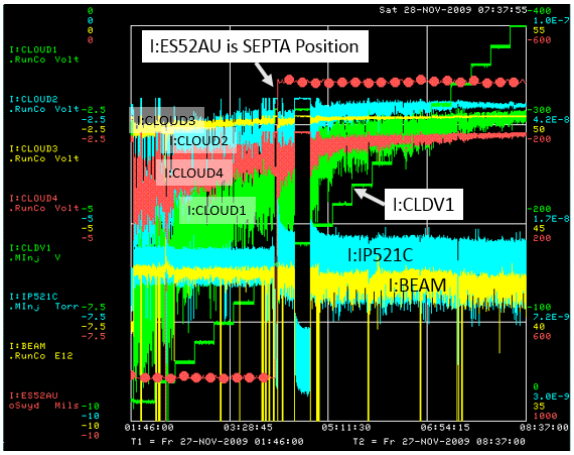
I:ES52AU is SEPTA Position
I:CLOUD3
I:CLOUD2
I:CLOUD4
I:CLOUD1
I:CLDV1
I:IP521C
I:BEAM

Figure 4:

6 Conclusion

In conclusion, this paper offers a simple mechanism to determine the amount of energy the beam can deposit into a wire. Since the septa consist of more than just a wire, more work is needed to better understand the impact on the system. As wires break from the ends, increased electric fields within the Septa tanks can lead to increased forces and increased rates of wire breakage. The other two mechanisms, RF heating and residual gas interactions, will require more testing and or simulation to determine whether they can be contributing to wire breakage. As the Main Injector intensity increases both of these effects will become more relevant.

It should be noted that this document ignores mechanical considerations which could also cause this wire breakage and likely many other effects still unknown to the author.

References

[1] J. Fowler, *http://physics.princeton.edu/ phy209/week2/bethe_formula.pdf* Princeton 2009

[2] N. Nakamura et al. *Particle Data Group*, J. Phys. G 37, 075021 2010 and 2011 partial update for the 2012 edition.

[3] Michael Backfish, *MiniBooNE Resistive Wall Current Monitor*, Fermilab TM-2556-AD, Batavia, Il 2013

[4] NIST, *http://physics.nist.gov/PhysRefData/Star/Text/PSTAR.html*

[5] F. Roncarolo, F. Caspers, B. Dehning, E. Jensen, J. Koopman, J.F. Malo. *Cavity Mode Related Wire Breaking of the SPS Wire Scanners and Loss Measurements of Wire Materials*, CERN, 2003

[6] E. Piselli, O.E. Berrig, F. Caspers, B. Dehning, J. Emery, M. Hamani, J. Kuczerowski, B. Salvant, R. Sautier, R. Veness, C. Vuitton, C. Zannini. *CERN-SPS Wire Scanner Impedance and Wire Heating Studies*, IBIC 2014

[7] M. Backfish. "Electron Cloud in Steel Beam Pipe vs Titanium Nitride Coated and Amorphous Carbon Coated Beam Pipes in Fermilab's Main Injector"', Indiana University and Fermilab, 2013